

Type I Cytokines Synergize with Oncogene Inhibition to Induce Tumor Growth Arrest

Nicolas Acquavella¹, David Clever¹, Zhiya Yu¹, Melody Roelke-Parker², Douglas C. Palmer¹, Liqiang Xi¹, Holger Pflücke¹, Yun Ji³, Alena Gros¹, Ken-ichi Hanada¹, Ian S. Goldlust^{4,5}, Gautam U. Mehta¹, Christopher A. Klebanoff¹, Joseph G. Crompton^{1,5}, Madhusudhanan Sukumar¹, James J. Morrow^{6,7}, Zulmarie Franco¹, Luca Gattinoni³, Hui Liu², Ena Wang⁹, Francesco Marincola⁹, David F. Stroncek⁸, Chyi-Chia R. Lee¹, Mark Raffeld¹, Marcus W. Bosenberg¹⁰, Rahul Roychoudhuri¹, and Nicholas P. Restifo¹

Abstract

Both targeted inhibition of oncogenic driver mutations and immune-based therapies show efficacy in treatment of patients with metastatic cancer, but responses can be either short lived or incompletely effective. Oncogene inhibition can augment the efficacy of immune-based therapy, but mechanisms by which these two interventions might cooperate are incompletely resolved. Using a novel transplantable BRAF^{V600E}-mutant murine melanoma model (SB-3123), we explored potential mechanisms of synergy between the selective BRAF^{V600E} inhibitor vemurafenib and adoptive cell transfer (ACT)-based immunotherapy. We found that vemurafenib cooperated with ACT to delay melanoma progression without significantly affecting tumor infiltration or effector function of endogenous or adoptively transferred CD8⁺ T cells, as previously observed. Instead, we found that the T-cell

cytokines IFN γ and TNF α synergized with vemurafenib to induce cell-cycle arrest of tumor cells *in vitro*. This combinatorial effect was recapitulated in human melanoma-derived cell lines and was restricted to cancers bearing a BRAF^{V600E} mutation. Molecular profiling of treated SB-3123 indicated that the provision of vemurafenib promoted the sensitization of SB-3123 to the anti-proliferative effects of T-cell effector cytokines. The unexpected finding that immune cytokines synergize with oncogene inhibitors to induce growth arrest has major implications for understanding cancer biology at the intersection of oncogenic and immune signaling and provides a basis for design of combinatorial therapeutic approaches for patients with metastatic cancer.

Cancer Immunol Res; 3(1); 37–47. ©2014 AACR.

See related commentary by Riddell, p. 23

Introduction

More than 50% of patients with metastatic melanoma have tumors driven by oncogenic BRAF^{V600E} mutations, which promote aberrant cell growth through constitutive activation of the MAPK pathway (1, 2). Inhibition of the BRAF^{V600E} oncoprotein can mediate profound tumor regression in a majority of patients, but the duration of these benefits is usually transient due to the emergence of drug-resistant tumors (3–5). Adoptive cell transfer (ACT) of autologous tumor-infiltrating lymphocytes can induce tumor regression,

but complete responses are only observed in a subset of patients with melanoma (6, 7). Treatment of patients with combinations of these two therapeutic modalities is conceptually promising but requires a fundamental understanding of potential mechanisms by which the two strategies might cooperate to induce tumor regression.

The combined use of the selective BRAF^{V600E} inhibitor vemurafenib with ACT results in augmented antitumor response (8, 9), but investigations into the mechanisms by which the two therapeutic modalities may synergize have focused on augmentation

¹Surgery Branch, Center for Cancer Research, National Cancer Institute (NCI), US National Institutes of Health (NIH), Bethesda, Maryland. ²Leidos Biomedical Research, Inc., Frederick National Laboratory for Cancer Research, Frederick, Maryland. ³Experimental Transplantation and Immunology Branch, Center for Cancer Research, National Cancer Institute (NCI), US National Institutes of Health (NIH), Bethesda, Maryland. ⁴Division of Preclinical Innovation, U.S. National Institutes of Health Chemical Genomics Center, National Center for Advancing Translational Sciences, Rockville, Maryland. ⁵Cancer Research United Kingdom Cambridge Institute, University of Cambridge, Li Ka Shing Centre, Cambridge, United Kingdom. ⁶Department of Pathology, Case Western Reserve University, Cleveland, Ohio. ⁷Department of Genetics & Genome Sciences Case Western Reserve University, Cleveland, Ohio. ⁸Department of Transfusion Medicine, Cell Processing Section, National Institutes of Health (NIH), Bethesda, Maryland. ⁹Sidra Medical and Research Center, Doha, Qatar. ¹⁰Department of Dermatology, Yale University School of Medicine, New Haven, Connecticut.

Note: Supplementary data for this article are available at Cancer Immunology Research Online (<http://cancerimmunolres.aacrjournals.org/>).

N. Acquavella and D. Clever contributed equally to this article.

Current address for N. Acquavella: Sylvester Comprehensive Cancer Center, Miller School of Medicine, University of Miami, Miami, Florida.

Current address for Z. Franco: Federal Drug Administration (FDA), Center for Biologics Evaluation and Research (CBER), 5516 Nicholson Lane, Kensington, Maryland.

Corresponding Authors: Nicholas P. Restifo, National Institutes of Health, National Cancer Institute, Building 10/Room 3-6257, Bethesda, MD 20892. Phone: 30-14-96-4904; Fax: 30-14-51-6949; E-mail: restifo@nih.gov; Nicolas Acquavella, nacquavella@miami.edu; and David Clever, cleverdc@mail.nih.gov

doi: 10.1158/2326-6066.CIR-14-0122

©2014 American Association for Cancer Research.

of host immune responses in the presence of BRAF inhibition (10–14). There is a strong precedent established by Kaplan and colleagues (15) indicating an essential role for the effector cytokine IFN γ in the prevention of tumorigenesis (15, 16). In addition, recent observations indicate that the T-cell-expressed cytokines IFN γ and TNF α exert direct antiproliferative effects on cancer cells through induction of cellular senescence (17). This led us to ask whether T-cell effector cytokines produced by adoptively transferred cells could synergize with vemurafenib to induce growth arrest.

To evaluate this, we constructed a melanoma cell line model designated SB-3123, which enables investigation of the interplay between oncogene inhibition and adaptive immunity both *in vitro* and upon orthotopic transfer into syngeneic immunocompetent hosts. Using this model, we found that ACT cooperates with vemurafenib to cause enhanced regression of melanoma, but this effect was not dependent upon enhanced infiltration or function of endogenous or adoptively transferred cells within tumors. Instead, we observed that the T-cell effector cytokines IFN γ and TNF α synergized with vemurafenib to directly induce cell-cycle arrest of SB-3123 melanoma cells *in vitro*. The combination treatment regimen of vemurafenib and effector cytokines reduced proliferative capacity beyond single-agent treatment also in human melanoma-derived cell lines and was restricted to cancers bearing a BRAF^{V600E} mutation. This mechanism, thus, may not be exclusively model specific and could be applicable in a broad variety of BRAF^{V600E}-mutant melanoma tumors. Mechanistically, molecular profiling of treated SB-3123 indicated that the provision of vemurafenib promoted the sensitization of SB-3123 to the antiproliferative effects of T-cell cytokines. The unexpected finding that immune cytokines synergize with oncogene inhibitors to induce growth arrest has major implications for understanding cancer biology at the intersection of oncogenic and immune signaling and provides a basis for design of combinatorial therapeutic approaches for patients with metastatic cancer.

Materials and Methods

Cell lines

The SB-3123_p cell line was derived from spontaneously arising melanoma in a female *Tyr::CreER; BRAF^{CA/CA}; PTEN^{lox4-5/lox4-5}; CTNNB1^{loxex3/loxex3}* transgenic mouse (18–22). The tumor was initially divided into small pieces and then implanted onto C57BL/6 female mice. Growing tumors were serially implanted onto C57BL/6 mice and after the second *in vivo* passage were minced and seeded under tissue culture conditions to derive the SB-3123_p cell line. B16 (H-2^b) is a BRAF wild-type (WT) murine melanoma cell line, and A375 is a BRAF^{V600E}-mutant human melanoma cell line, both obtained from the NCI tumor repository. The BRAF^{V600E}-mutant human melanoma UACC-62 cell line was a gift from Dr. Susan Bates (Medical Oncology Branch, NCI, Bethesda, MD). MC38 (H-2^b) is a colon cancer murine cell line obtained from the NCI tumor repository. Mouse Melan-a cells were a gift from Dr. Thomas Hornyak (University of Maryland School of Medicine, Baltimore, MD). Patient-derived, pathology-confirmed melanoma cell lines used in this study were generated from patients with metastatic, pathology-confirmed melanoma receiving treatment under Institutional Review Board-approved clinical protocols in the Surgery Branch of the NCI. Informed consent was obtained from all subjects. Melanoma cell lines grew from enzymatically or mechanically dispersed cells

or from 1- to 3- μ m tumor fragments that were cultured in 24-well plates (Corning 3524), one fragment or 1×10^6 cells/mL in 2 mL/well of RPMI-1640 medium (Lonza), supplemented with 10% heat-inactivated FBS (Hyclone, Defined) and 100 U/mL of penicillin, 100 μ g/mL of streptomycin, and 10 μ g/mL of Gentamicin (Lonza). The established cell lines grew as monolayer cultures. Genomic characterization of patient-derived melanoma cell lines was performed through exome sequencing, as previously described (22). The SB-3123, A375, B16, and UACC-62 cells were maintained in culture media composed of DMEM (Life Technologies) with 10% heat-inactivated FBS (Sigma), 1% GlutaMAX (Life Technologies), 1% (v/v) penicillin/streptomycin (Life Technologies), 1% Eagle's Minimum Essential Medium (MEM) nonessential amino acids (Life Technologies), 1% sodium pyruvate (Life Technologies), and 0.1% 2-mercaptoethanol (55 mmol/L; Life Technologies) in 5% CO₂ at a constant temperature (37°C) and humidity. Trophic factor-deficient media consisted of DMEM supplemented only with 1% GlutaMAX, 1% (v/v) penicillin/streptomycin, 1% MEM nonessential amino acids, 1% sodium pyruvate and 0.1% 2-mercaptoethanol. Melan-a cells were cultured in RPMI-1640 culture media (Life Technologies) with 5% heat-inactivated FBS, 0.1% phorbol 12-myristate 13-acetate (PMA; Sigma), 1% (v/v) penicillin/streptomycin and 1% GlutaMAX. All cell lines used were confirmed to be Mycoplasma free. No additional validation assay was performed.

Immunoblot analysis

Western blot analysis was performed using standard protocols. Whole-cell lysates were prepared using RIPA lysis buffer (Thermo Fisher Scientific). Proteins were separated by SDS-PAGE, followed by standard immunoblot analysis using phospho-Erk 1/2, total Erk 1/2, PTEN (all from Cell Signaling Technology), GAPDH (Millipore), V5 (Life Technologies), and β -actin (Santa Cruz Biotechnology). The expression of gp100 was detected using α -PEP13 antisera (gift from Dr. Vincent Hearing, NCI, Bethesda, MD).

Viability assays

Cells were seeded in a 96-well flat-bottom plate at a density of 2.0 to 2.5×10^3 cells per well and allowed to adhere for 24 hours in complete media. The following day, cells were treated with DMSO vehicle control and increasing concentrations of vemurafenib (PLX4032; Chemie Tek) in triplicate and cells were incubated for 72 hours. In all 8×8 matrix experiments, SB-3123 were treated with 0.1% BSA vehicle control, vemurafenib (0–16 μ mol/L), mouse IFN γ (0.8–51.2 ng/mL), TNF α (0.08–5.12 ng/mL), human IFN γ (0.4–100 ng/mL), TNF α (0.04–10 ng/mL; PeproTech) and cells were incubated for 96 hours. Cells were analyzed using the CellTiter-Glo Luminescent Cell Viability Assay according to the manufacturer's protocol (Promega).

In vitro activation of Pmel-1 CD8⁺ T cells

To generate antigen-specific CD8⁺ T cells for ACT, splenocytes from Pmel-1 (Thy1.1⁺) T-cell receptor (TCR) transgenic mice were depleted of erythrocytes by ACK lysis and cultured in complete media with 30 IU/mL of recombinant human IL2 (rhIL2; Novartis) in the presence of 1 μ mol/L hgp100₂₅₋₃₃ of peptide and expanded for 5 days.

Retroviral transduction of SB-3123 to express mouse gp100

Full-length mouse gp100 cDNA was amplified from B16 F10 melanoma cells, and cDNA was cloned into the gamma-

retrovirus vector pMSGV1 V5 IRES (internal ribosome entry site) Bsr (blastidicin S resistance) so that the V5 epitope tag was added to the C-terminus of gp100. To retrovirally transduce SB-3123, the retrovirus producer cell line 293gp was transiently transfected with pMSGV1 gp100 V5 IRES Bsr and pMDG that encoded the VSVE envelope gene. Transduced cells were selected by culture in Blastidicin S, and the gp100 expression was confirmed by qRT-PCR, Western blot analysis using anti-V5 tag antibody.

***In vivo* antitumor efficacy studies with vemurafenib**

C57BL/6 female mice ($n = 5$ for all groups), ages 6 to 8 weeks and weighing approximately 19 to 20 g, were injected s.c. with 3 to 5×10^5 SB-3123_p, B16, or SB-3123 melanoma cells in 100 μ L of 1 \times PBS into the abdomen. Tumors were allowed to reach approximately 60 mm² before the initiation of treatment. Vemurafenib tablets were crushed using a mortar and pestle, and the powder was suspended at the desired concentration in an aqueous vehicle containing 2% Klucel LF (Hydroxypropylcellulose; Ashland) and adjusted to pH 4 with dilute HCL. Vemurafenib was administered uninterruptedly by oral gavage on a daily basis.

Adoptive transfer of Pmel-1 CD8⁺ T cells and tumor treatment

C57BL/6 female mice ($n = 5$ for all groups), ages 6 to 8 weeks, were injected s.c. with 3 to 5×10^5 gp100-transduced SB-3123 cells in 100 μ L of 1 \times PBS into the abdomen. Mice with established tumors were treated with i.v. injections of 2.5×10^6 *in vitro*-activated Pmel-1 (Thy1.1⁺) splenocytes for 5 days and vaccinated by i.v. injection of 2×10^7 plaque-forming units of recombinant vaccinia virus encoding hgp100 (rVVhgp100) followed by 2 daily i.p. injections of rhIL2 (150,000 IU rhIL2 in $\times 1$ PBS, for 3 days). Collectively, this treatment is designated as ACT. Treated mice received 600 cGy of sublethal irradiation before transfer of Pmel-1 CD8⁺ T cells.

Intracellular IFN γ and TNF α assays

All FACS antibodies were purchased from BD Biosciences, except antibody to mouse CD8 α (eBioscience). A leukocyte activation cocktail containing phorbol myristate acetate and ionomycin (BD Biosciences) was used to stimulate T cells for intracellular cytokine staining. Flow-cytometry acquisition was performed on a BD LSR II flow cytometer.

***In vitro* proliferation assays and cell-cycle analysis**

After treatment, SB-3123 proliferation and cell-cycle analysis was measured by the APC-BrdUrd Flow Kit according to the manufacturer's protocol (BD Pharmingen). The following cell-cycle phases were determined as a percentage of the total population: sub-G₁ (apoptotic cells), G₁-G₀ (2n, BrdUrd-negative), S (2n to 4n, BrdUrd-positive), and G₂-M phase (4n, BrdUrd-negative). Flow-cytometry acquisition was performed on a BD Canto II flow cytometer.

Analysis of *in vitro* synergy

The Loewe synergy analysis was performed on data shown in Supplementary Fig. S7. The analysis was carried out using the Combenefit software version 1.22 (<http://www.cruk.cam.ac.uk/research-groups/jodrell-group/combenefit>), which relies on the Loewe additivity model (24).

Microarray analysis

Total RNA (100 ng), extracted as previously described, was amplified using the Ovation Pico WTA System V2 (NuGEN), according to the manufacturer's instructions. Briefly, first-strand cDNA was synthesized using the SPIA-tagged random and oligo-dT primer mix in 10 μ L reactions after denaturation and incubated at 65°C for 2 minutes, and priming at 4°C was followed by extension at 25°C for 30 minutes, 42°C for 15 minutes, and 77°C for 15 minutes. Second-strand cDNA synthesis of fragmented RNA was performed using DNA polymerase at 4°C for 1 minute, 25°C for 10 minutes, 50°C for 30 minutes, and 80°C for 20 minutes. 5' double-stranded cDNA was used as the template for isothermal single-strand cDNA amplification following a cycle of DNA/RNA primer binding, DNA replication, strand displacement, and RNA cleavage at 4°C for 1 minute, 47°C for 75 minutes, and 95°C for 5 minutes in total 100 μ L reaction. Samples were fragmented and biotinylated using the Encore Biotin Module (NuGEN) according to the manufacturer's instructions. Biotinylated cDNA was then hybridized to Mouse Gene 1.0 ST arrays (Affymetrix) overnight at 45°C and stained on a Genechip Fluidics Station 450 (Affymetrix), according to the respective manufacturer's instructions. Arrays were scanned on a GeneChip Scanner 3000 7G (Affymetrix). Global gene-expression profiles rank ordered by relative fold-change values were analyzed by using Gene set enrichment analysis software (Broad Institute, MIT). *P* values were calculated using the Student *t* test using Partek Genomic Suite after Robust Multiarray Average (RMA) normalization.

Statistical analyses

In vitro assays were repeated at least three times and *in vivo* studies at least two times. Mean comparisons were conducted by using an unpaired *t* test. For *in vivo* studies, the products of perpendicular tumor diameters were plotted as the mean \pm SEM for each data point, and groups were compared using the Wilcoxon rank-sum test. The log-rank test was used to analyze survival curves. *P* values of ≤ 0.05 were considered statistically significant. All statistical analyses were calculated using Prism 5 GraphPad software (GraphPad Software Inc.).

Accession numbers

The microarray data are available in the Gene Expression Omnibus (GEO) under accession number GSE62249.

Results

SB-3123 murine melanoma becomes resistant to prolonged vemurafenib therapy

To better model human melanoma tumors, we derived a syngeneic transplantable cell line from tumors arising in a BRAF^{V600E}-mutant autochthonous tumor model that has been previously described (25, 26). We observed that this model, consistent with its molecular architecture, was sensitive to vemurafenib treatment (Supplementary Fig. S1A and S1B). The resultant murine melanoma cell line (SB-3123_p) was transplantable into syngeneic hosts and exhibited key molecular characteristics consistent with BRAF^{V600E} melanoma (Supplementary Fig. S1C-S1H) as assessed by mutation-specific primers (Supplementary Fig. S2). ERK activity was inhibited in a vemurafenib dose-dependent manner in SB-3123_p cells at levels comparable with human BRAF^{V600E}-mutant melanoma

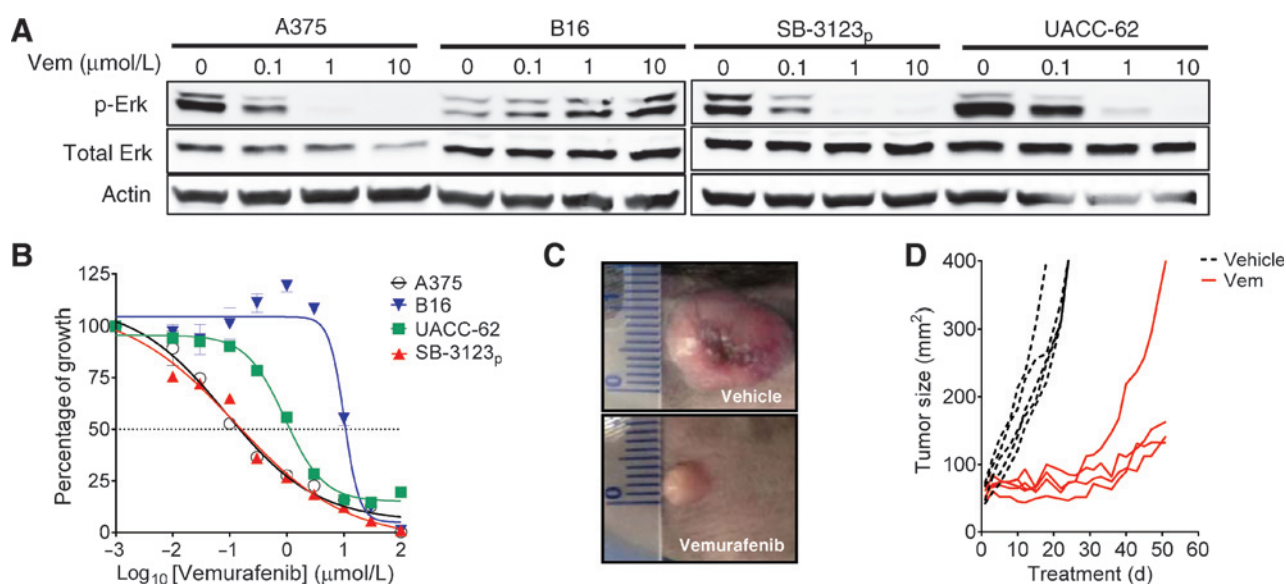


Figure 1. BRAF^{V600E}-mutant melanoma becomes resistant to vemurafenib (Vem). A, SB-3123_p cells and corresponding controls were treated with increasing concentrations of vemurafenib and the effects on MAPK signaling were determined by immunoblotting for p-ERK1/2 at 1 hour. Total ERK1/2 and *Actin* were used as loading controls. B, cell viability and IC₅₀ determination of BRAF^{V600E}-mutant SB-3123_p murine melanoma cells, BRAF WT B16 murine melanoma cells and BRAF^{V600E}-mutant A375 and UACC-62 human melanoma cells were treated with vemurafenib at the indicated concentrations for 72 hours (relative to DMSO-treated controls; mean ± SEM, *n* = 3). C, representative SB-3123_p tumors established on a C57BL/6 host treated with vehicle or 50 mg/kg of vemurafenib once daily by oral gavage for 2 weeks. D, prolonged dosing of SB-3123_p-bearing C57BL/6 mice with vehicle and 50 mg/kg of vemurafenib once daily by oral gavage for 50 days leads to the emergence of vemurafenib-resistant tumors (mean tumor size ± SEM; *n* = 5).

cells, whereas it remained unaffected in WT BRAF-expressing B16 murine melanoma cells (Fig. 1A). The 50% inhibition concentration (IC₅₀) of SB-1323_p was similar to the highly sensitive A375 human melanoma cell line (Fig. 1B). Furthermore, the antitumor effect of vemurafenib was BRAF^{V600E} specific because treatment of SB-3123_p-bearing immunocompetent mice resulted in substantial inhibition of tumor growth (Fig. 1C and Supplementary Fig. S3A and S3B) in contrast with treatment of implanted B16 melanoma tumors (Supplementary Fig. S4A and S4B).

Objective tumor responses in patients with BRAF^{V600E} melanomas treated with BRAF inhibitors are short-lived, and tumors eventually progress due to the development of drug-resistant disease (26). This phenomenon was recapitulated in SB-3123_p melanomas because tumor recrudescence emerged in all mice continuously treated with vemurafenib following approximately 1 month of therapy (Fig. 1D). Thus, SB-3123 is a novel murine orthotopic melanoma model that recapitulates key molecular characteristics of a majority of human melanoma tumors, including initial sensitivity to vemurafenib therapy and emergence of drug resistance *in vivo*.

Vemurafenib complements efficacy of CD8⁺ T-cell immunotherapy without augmenting CD8⁺ T-cell immunity

Recrudescence of SB-3123_p melanomas led us to inquire whether vemurafenib would synergize with ACT to induce more durable tumor regression. We therefore generated an SB-3123_p-derived cell line called SB-3123 that expresses the model self-antigen murine gp100 that is recognized by Pmel-1 TCR-transgenic CD8⁺ T cells (Supplementary Fig. S5). We found that ACT using tumor-reactive Pmel-1 CD8⁺ T cells cooperated with vemurafenib administration to delay the emergence of drug-resistant

melanoma (Fig. 2A and Supplementary Fig. S6) and translated into a significant survival advantage (Fig. 2B and Supplementary Fig. S6), as has been demonstrated in other model systems (8, 9). Because the superior combined effect of concurrent vemurafenib administration has previously been attributed to augmentation of CD8⁺ T-cell-intrinsic antitumor immunity, we evaluated adoptively transferred and endogenous CD8⁺ T-cell responses in SB-3123 tumor-bearing mice treated or untreated with vemurafenib. Surprisingly, we found no significant differences in the function or number of adoptively transferred (Thy1.1⁺) or endogenous splenic and tumor-infiltrating CD8⁺ T cells (Fig. 3A–E). Thus, in the SB-3123 tumor model, ACT cooperates with vemurafenib to induce enhanced disease regression, but this is not attributable to the potentiation of systemic endogenous or transferred immune responses.

IFN γ and TNF α synergize with vemurafenib to induce SB-3123 tumor growth arrest

The dramatic outcome of concurrent vemurafenib and ACT in delaying SB-3123 tumor progression, despite causing no observable differences in T-cell recruitment and effector function in this model, suggested an alternative mode of cooperation between vemurafenib and ACT. Multiple reports have indicated that T-cell effector cytokines can directly induce tumor cell-cycle arrest (17, 28, 29). In addition, the antitumor effects of vemurafenib administration require intact host IFN γ production, as IFN γ depletion reduced tumor responsiveness to vemurafenib (13). We thus hypothesized that the provision of T-cell effector cytokines from adoptively transferred cells synergized with vemurafenib at a tumor cell-intrinsic level to promote reduced proliferation and superior tumor growth control. To test this hypothesis, we evaluated whether effector cytokines synergize with

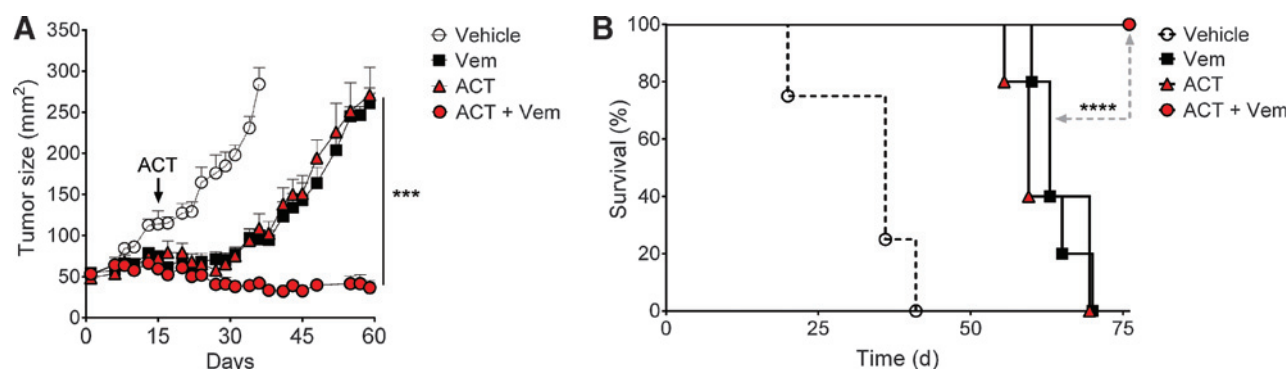


Figure 2.

Concurrent vemurafenib therapy is required for sustained tumor growth control. A, SB-3123-bearing C57BL/6 mice were treated with vehicle or vemurafenib (Vem) for 60 days. Two treatment groups received vemurafenib for 15 days followed by ACT (black arrow). ACT consisted of the following: sublethal irradiation, 2.5×10^6 *in vitro*-activated Pmel-1 CD8⁺ T cells, 2×10^7 plaque-forming units of recombinant vaccinia virus encoding hgp100 (rVVhgp100) and two daily i.p. injections of rhlL2 (150,000 IU rhlL2). Following ACT, vemurafenib was either discontinued (ACT) or continued until day 60 (ACT + Vem). Mean tumor size \pm SEM is shown ($n = 5$). B, survival curves according to treatment in A; ***, $P = 0.0001$, by the Wilcoxon rank-sum test; ****, $P \leq 0.0001$, by log-rank statistics.

vemurafenib to inhibit SB-3123 growth *in vitro*. Although both vemurafenib and IFN γ /TNF α treatment inhibited tumor cell viability and proliferation when individually added to SB-3123 cell cultures at high doses, their effect was strikingly synergistic when IFN γ /TNF α and vemurafenib were combined at lower doses, which individually produced relatively minimal effects (Fig. 4A–D and Supplementary Figs. S7 and S8). Upon cell-cycle analysis, 84% of untreated SB-3123 cells were in S phase and 12% in G₁–G₀, indicative of rapid proliferative growth. This was mildly altered at selected suboptimal doses of cytokines and vemurafenib, but altered significantly when these agents were combined at identical doses, such that 37% of cells were arrested in G₁–G₀ and 31% were in S phase, with a significant increase in the G₁–S ratio upon combination treatment (Fig. 4E and F and Supplementary Fig. S9).

The combinatorial effects of vemurafenib and effector cytokines are restricted to BRAF-mutant murine and human tumors

To evaluate whether the synergistic relationship of vemurafenib and effector cytokines in inducing SB-3123 growth arrest was dependent upon the presence of a tumor-specific BRAF^{V600E} mutation, we treated BRAF^{WT} (B16) and BRAF-mutant (SB-3123) murine melanoma cells with each agent alone or with a combination of vemurafenib and IFN γ /TNF α in an *in vitro* dose-escalation matrix. Although both cell lines were moderately sensitive to T-cell effector cytokines at the highest doses evaluated, vemurafenib inhibited cell growth exclusively in the BRAF^{V600E}-mutant SB-3123. Importantly, synergy between vemurafenib and IFN γ /TNF α in inhibiting cell growth was observed only in BRAF^{V600E}-mutant SB-3123 cells and not in BRAF-WT B16 cells. We concluded that the cooperative effect of vemurafenib and IFN γ /TNF α was mediated in a BRAF^{V600E} mutation-dependent manner (Fig. 5A and Supplementary Fig. S10).

To determine whether the combinatorial effect of vemurafenib and effector cytokine treatment was restricted to the SB-3123 model or represents a more generally applicable mechanism in human melanoma, we treated low-passage BRAF^{WT} and BRAF^{V600E} patient-derived melanoma cell lines *in vitro* and observed superior growth inhibition with combination treatment

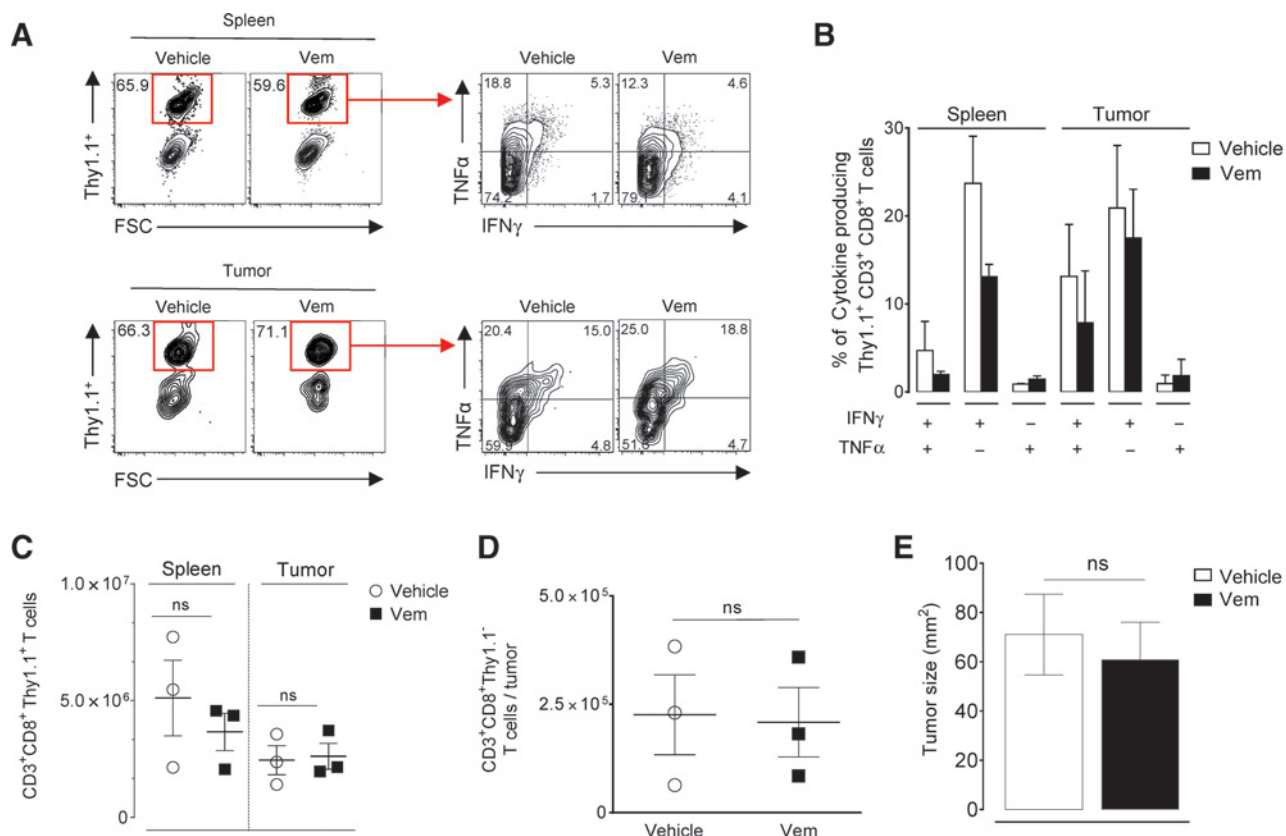
relative to single-agent treatment. This cooperation was seen only in the human BRAF^{V600E}-mutant melanoma cell lines but not in the BRAF WT cells (Fig. 5B and Supplementary Fig. S11). This indicates that the biologic cooperation between vemurafenib and effector cytokines is BRAF^{V600E} mutation-dependent and not restricted to murine melanoma.

Vemurafenib augments an effector cytokine-induced transcriptional program

We next investigated the molecular mechanisms by which vemurafenib and effector cytokines synergized to promote cell-cycle arrest of SB-3123. T-cell effector cytokines IFN γ and TNF α have been shown to have direct antiproliferative effects in tumors (17, 28, 29). Considering the surprising finding that in the SB-3123 model concurrent vemurafenib administration did not affect cytokine production in adoptively transferred CD8⁺ T cells, we were led to hypothesize that the provision of vemurafenib, rather than enhancing T-cell cytokine production, rendered SB-3123 more sensitive to T-cell cytokines. To gain insight into this hypothesis, we performed whole transcriptome analysis on SB-3123 cells grown *in vitro* under control, vemurafenib only, IFN γ /TNF α only, or combination vemurafenib + IFN γ /TNF α treatment conditions. Each treatment caused a unique gene-expression signature in SB-3123 with differential expression of greater than 1,000 transcripts relative to untreated cells (Fig. 6A; Supplementary Tables S1–S5, $P < 0.01$). The combination of vemurafenib + IFN γ /TNF α promoted the differential expression of 1,954 gene transcripts normalized to those of untreated cells that were distinct from transcripts induced in either of the single-agent treatment groups (Fig. 6B; Supplementary Tables S2–S5). This indicated that the combination treatment promoted genetic changes beyond the summation of changes induced by either single-agent therapy.

To investigate the genetic changes that occurred upon combination treatment beyond the changes induced by either vemurafenib or IFN γ /TNF α alone, we performed gene set enrichment analysis (GSEA) on the transcripts from the combination treatment group rank ordered by relative fold-change to transcripts from either IFN γ /TNF α -only or vemurafenib-only treatment groups [(Vem + IFN γ /TNF α vs. IFN γ /TNF α only) or

Acquavella et al.

**Figure 3.**

CD8⁺ T-cell effector responses are not compromised by treatment with vemurafenib. A, representative flow cytometry of adoptively transferred Thy1.1⁺ CD8⁺ Pmel transgenic T cells and effector cytokine production in spleens (top) and SB-3123 tumors (bottom) 5 days following adoptive T-cell transfer. IFN γ and TNF α production were measured after a short Pmel splenocyte reestimulation with a leukocyte activation cocktail containing phorbol myristate acetate and ionomycin. B, histograms indicating expression of indicated cytokines by Thy1.1⁺ Pmel-1 CD8⁺ T cells in spleens and tumors at 5 days following adoptive transfer. Differences are not statistically significant for any group. C, absolute number of adoptively transferred CD3⁺ CD8⁺ Thy1.1⁺ Pmel-1 T cells in spleens and tumors at 5 days following T-cell transfer. D, absolute number of CD3⁺ CD8⁺ Thy1.1⁻ endogenous T cells in SB-3123 tumors 5 days after T-cell transfer. E, SB-3123 tumor size at day 5 following T-cell transfer. ns, not statistically significant.

(Vem + IFN γ /TNF α vs. Vem only)]. Interestingly, both IFN- and TNF-responsive gene sets showed significant positive enrichment with the transcriptional changes specific to the combination treatment, even relative to IFN γ /TNF α alone-induced gene-expression changes (Fig. 7A; Supplementary Table S6 and S7). Vemurafenib treatment alone did not enrich IFN γ or TNF α gene sets (Supplementary Table S8). Taken together, this suggested that the provision of vemurafenib in the context of IFN γ /TNF α treatment sensitized SB-3123 to cytokine-induced genetic changes.

The GSEA of the combination treatment normalized to IFN γ /TNF α single-agent therapy showed negative enrichment, to a significant degree, of multiple cell-cycle-promoting gene sets (Fig. 7B; Supplementary Table S7). This result is consistent with the observed increase in the G₁-S ratio and reduction in proliferative capacity in SB-3123 treated with vemurafenib + IFN γ /TNF α *in vitro*. It is also consistent with delayed SB-3123 recrudescence observed *in vivo* with vemurafenib and ACT cotreatment.

We next directly investigated whether vemurafenib indeed sensitized SB-3123 melanoma cells to IFN γ /TNF α -induced gene-expression changes, as the GSEA data suggested. First, we identified 77 genes that showed significant upregulation

in IFN γ /TNF α -treated SB-3123 relative to control-treated cells (FC > 2.0, $P < 0.01$). We then tested for positive enrichment of these genes in SB-3123 cells receiving combination treatment relative to cells treated with IFN γ /TNF α alone. These analyses revealed positive enrichment with significant cytokine-responsive genetic changes, indicating an increased induction of the IFN γ /TNF α gene signature in SB-3123 upon vemurafenib + IFN γ /TNF α combination treatment (Supplementary Fig. S12).

To further demonstrate this, we evaluated under all treatment conditions the expression of the 20 most positively induced genes upon IFN γ /TNF α treatment relative to untreated SB-3123. Consistent with the enrichment results, we observed increased expression of cytokine-responsive genes in SB-3123 under vemurafenib + IFN γ /TNF α treatment conditions beyond the level of IFN γ /TNF α treatment alone (Fig. 7C).

We next performed a similar analysis to evaluate the expression of the most differentially expressed genes in SB-3123 following single-agent treatment with vemurafenib (Supplementary Table S10). Interestingly, the expression levels of the 20 most differentially expressed transcripts were not significantly different between vemurafenib single-agent treatment and vemurafenib + IFN γ /TNF α combination treatment (Fig. 7D). These data suggest

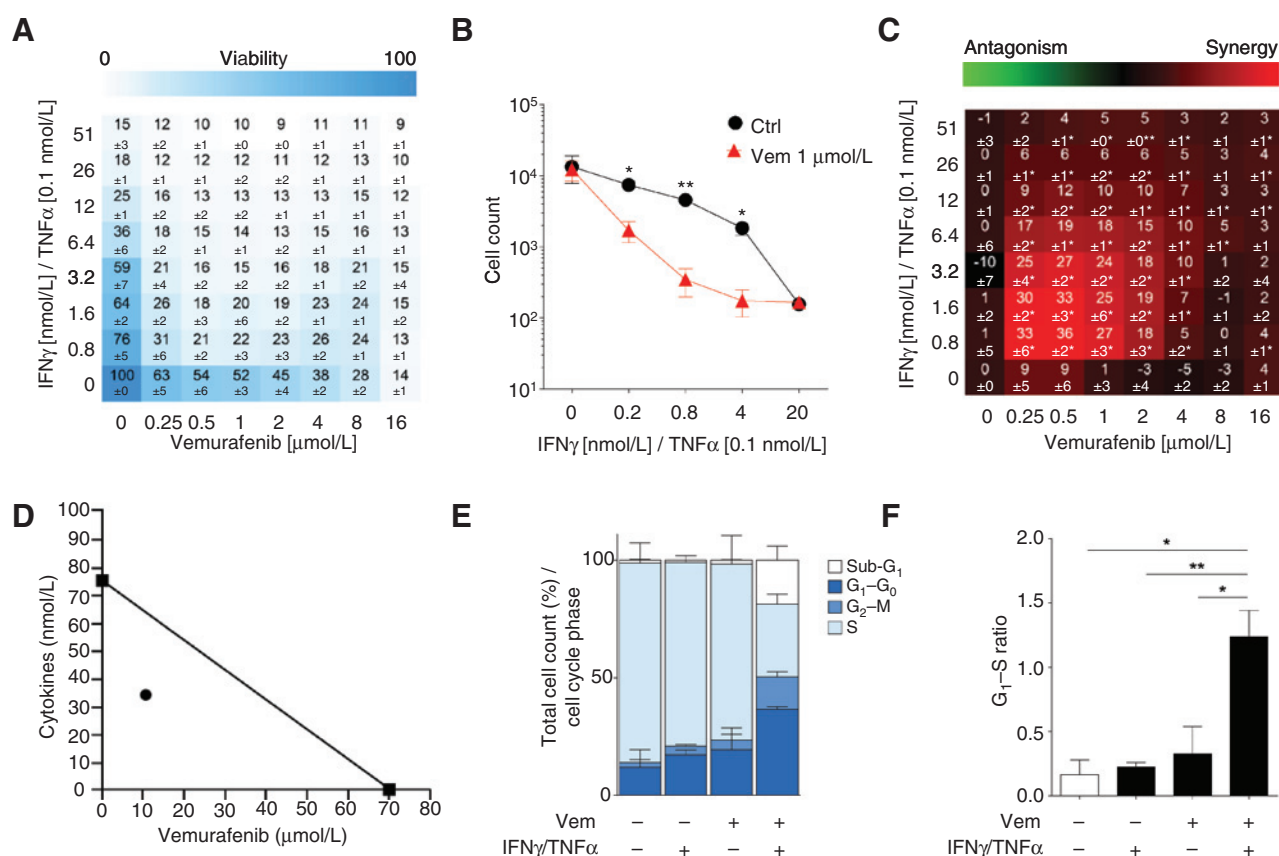


Figure 4. Vemurafenib (Vem) and T-cell effector cytokines synergize to induce cell-cycle arrest. A, viability of SB-3123 cells grown in indicated titrated doses of vemurafenib and IFN γ /TNF α (relative to DMSO-treated controls; mean \pm SEM, $n = 3$). B, absolute SB-3123 cell count after treatment with vemurafenib (1 μ mol/L) and increasing concentrations of IFN γ /TNF α for 96 hours. *, $P = 0.0234$; **, $P = 0.0074$; and *, $P = 0.0485$; unpaired t test. C, degree of synergy and antagonism as determined by the Loewe additivity model using data in A. D, isobologram analysis from our 8 \times 8 screen for the synergistic (black circle) drug combination of vemurafenib + IFN γ /TNF α ; $F_a = 0.9$. E, cell-cycle analysis; and F, the mean G $_1$ -S phase ratio of SB-3123 cells cultured in the presence or absence of vemurafenib, IFN γ /TNF α , or the combination (mean \pm SEM, $n = 3$); *, $P = 0.0363$; **, $P = 0.0082$; and *, $P = 0.0102$, by unpaired t test.

that, although provision of vemurafenib sensitized SB-3123 to effector cytokine-induced genetic changes, there was no enhancement of vemurafenib-induced changes by combination with IFN γ /TNF α .

Discussion

The lack of correspondence of traditional immunodeficient murine models of melanoma to clinical trial results (30, 31) and logistical challenges of solely using autochthonous tumor models

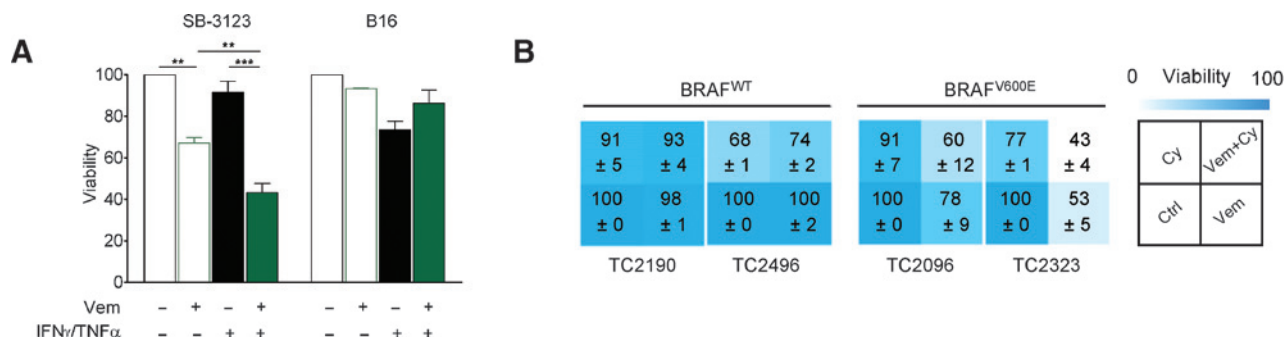


Figure 5. Vemurafenib and T-cell effector cytokines cooperate to inhibit growth of mouse and human melanoma in a BRAF^{V600E} mutation-dependent manner. A, viability of murine B16 and SB-3123 melanoma cells grown in vemurafenib (1 μ mol/L) and IFN γ /TNF α (2.4/0.24 ng/mL) relative to DMSO-treated controls; mean \pm SEM, ($n = 3$); ***, $P = 0.0005$; **, $P = 0.0030$; and ***, $P = 0.0013$. B, viability of patient-derived human melanoma cells treated with vemurafenib (2.5 μ mol/L) and IFN γ /TNF α (6.25/0.625 ng/mL) for 96 hours; (relative to DMSO-treated controls; mean \pm SEM, $n = 2$). Cy, IFN γ /TNF α .

Acquavella et al.

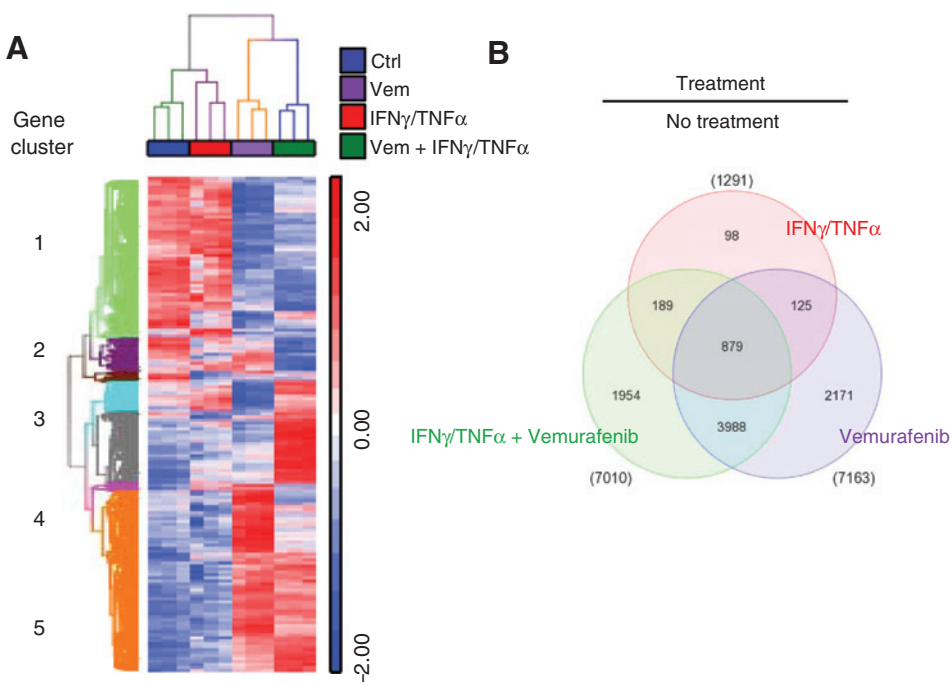


Figure 6. Vemurafenib (Vem) + IFN γ /TNF α combination treatment induces a unique gene-expression profile distinct from vemurafenib or IFN γ /TNF α single treatment. A, heatmap indicating global gene-expression profile of SB-3123 grown under indicated culture conditions. Heatmap includes all significantly expressed genes (one-way ANOVA, FDR corrected $P < 0.05$). Hierarchical clustering by Pearson correlation is shown, and gene lists of each cluster are available in Supplementary Tables S1–S5. B, analysis schematic and Venn diagram outlining number of genes differentially expressed ($P < 0.01$) between indicated treatment and control (Ctrl; no treatment).

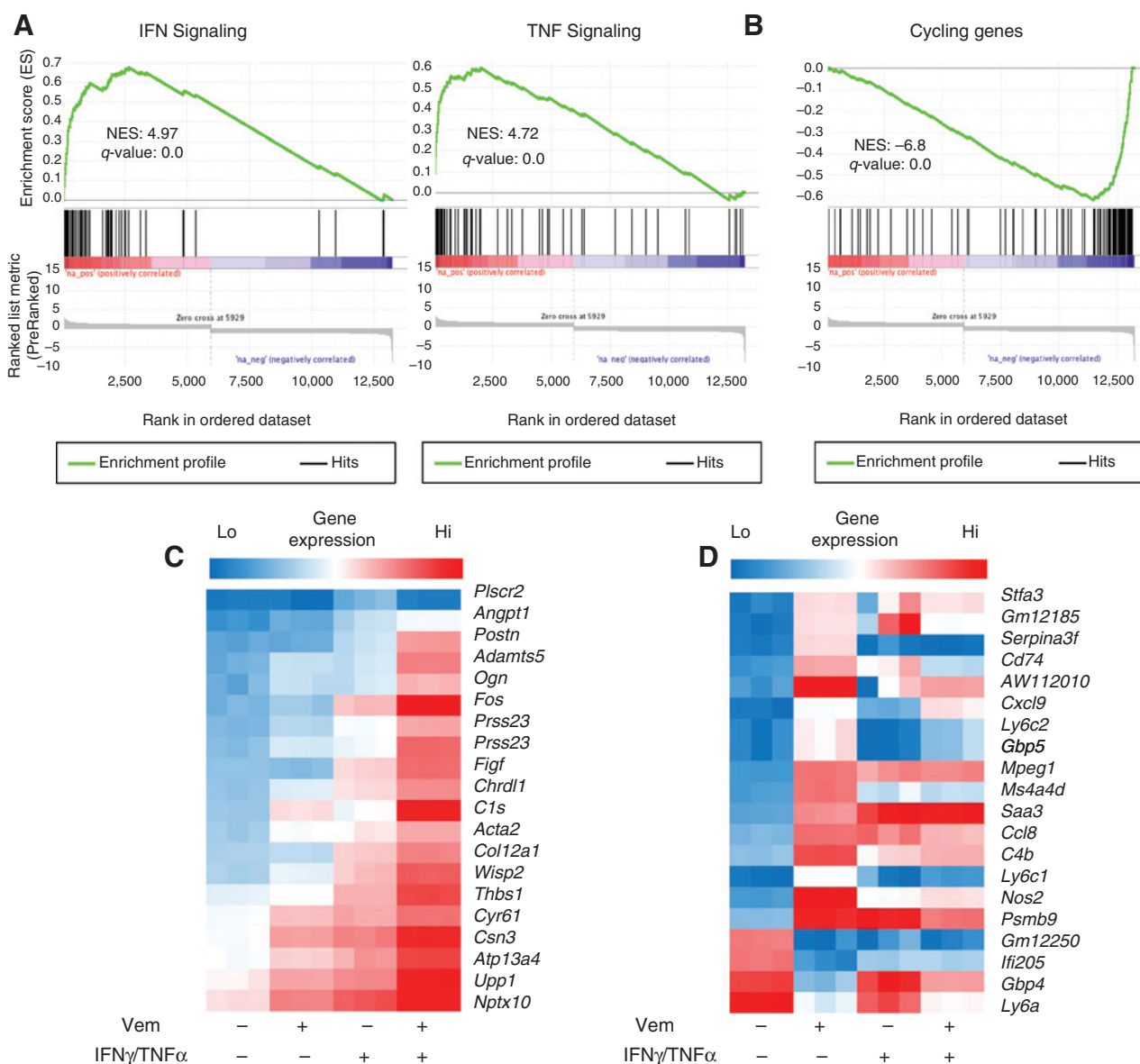
to test synergistic responses between vemurafenib and ACT (including through characterization using defined *in vitro* conditions) led us to develop the SB-3123 BRAF^{V600E} PTEN^{-/-} murine melanoma transplantable model that emulates a common genetic landscape in human melanoma. The presence of a heterozygous BRAF^{V600E} mutation occurring in a PTEN-deficient background in SB-3123 recapitulates one of the most common genetic profiles in human melanoma, accounting for approximately 44% of patients (32). Compared with other recently developed murine melanoma syngeneic transplantable cell lines (9, 33), the SB-3123 model system closely resembles the human circumstance, given its high *in vitro* and *in vivo* sensitivity to BRAF inhibition at clinically relevant drug exposures (34). More importantly, this model system permits the development of tumor resistance *in vivo* with prolonged vemurafenib exposure, recapitulating the clinical experience in patients treated with BRAF inhibitors (Fig. 1). Furthermore, the emergence of vemurafenib-resistant melanoma at different rates of progression in the SB-3123 model (Fig. 1D) recapitulates the heterogeneity observed in times to disease progression among patients treated with BRAF inhibitors and served to preclinically model a more realistic efficacy endpoint.

Using this model, we found that vemurafenib cooperated with ACT to induce enhanced tumor regression that was independent of an effect on endogenous and transferred immune responses as reported by others (35, 36). A potential explanation for this discrepancy may relate to the high affinity interaction between the transduced melanoma differentiation antigen (MDA) gp100 in SB-3123 and adoptively transferred Pmel-1 TCR-transgenic CD8⁺ T cells. In previous work, the upregulation of MDA by BRAF inhibition is the basis of enhanced T-cell recognition. However, mouse gp100 is not expressed under its physiologic promoter, making it insensitive to MITF (Microphthalmia-associated transcription factor) regulation (37). To evaluate vemurafenib and ACT cooperation, we engineered SB3123 to express gp100, and the resulting supraphy-

siologic expression of gp100 may lead to increased interaction with the adoptively transferred Pmel-1 T cells. This increased antigen–T-cell interaction may potentially mitigate any enhanced cytokine production with concurrent vemurafenib treatment, which has been observed when targeting antigens expressed at physiologic levels.

Nevertheless, the enhanced tumor regression observed in SB-3123 treated with vemurafenib and ACT prompted us to explore alternative mechanisms by which these two modalities cooperated, namely, by evaluating the molecular responses in SB-3123 upon exposure to vemurafenib and T-cell effector cytokines as single agents or in combination. We observed *in vitro* that the combination of vemurafenib + IFN γ /TNF α was more effective than single-agent therapy exclusively in BRAF^{V600E}-mutant mouse and human cell lines. This led us to postulate that vemurafenib may be rendering BRAF-mutant tumors more susceptible to the effects of T-cell cytokines. This hypothesis was supported by evaluation of the expression levels of IFN γ /TNF α treatment-responsive genes in SB3123 as revealed by whole-transcriptome analysis. These experiments indicated an increased IFN γ /TNF α genetic signature in SB-3123 treated with the combination of vemurafenib + IFN γ /TNF α , even beyond that with IFN γ /TNF α treatment alone. GSEA of the gene-expression profile of vemurafenib + IFN γ /TNF α -treated SB-3123 revealed a negative enrichment of the cell-cycle progression genes, which is consistent with the reduced growth kinetics and distinct cell-cycle profile in SB-3123 treated with this combinatorial regimen. Taken together, we propose that the provision of vemurafenib sensitized SB-3123 to T-cell effector cytokines and mediated reduced growth *in vitro*.

IFN γ has been well characterized as having antiproliferative effects and is a critical factor in controlling the induction and proliferation of cancer (15, 16, 28, 29, 38, 39). Recently, it has been established that the antitumor effects of vemurafenib require intact host IFN γ production (13). Our studies offer a potential

**Figure 7.**

Vemurafenib (Vem) sensitizes SB-3123 melanoma to the antiproliferative effects of T-cell effector cytokines. A and B, GSEA of fold-change gene expression in SB-3123 treated with vemurafenib (1 μ mol/L) + IFN γ /TNF α (2.4/0.24 ng/mL) compared with IFN γ /TNF α (2.4/0.24 ng/mL)-only treated SB-3123. Nonrandom positive enrichment of genes comprising the BROWNE_INTERFERON_RESPONSIVE_GENES and SANA_TNF_SIGNALING_UP gene sets (A) and nonrandom negative enrichment of the CHANG_CYCLING_GENES gene set (B) within the vemurafenib + IFN γ /TNF α -dependent gene expression profile in SB-3123 96 hours after treatment. C and D, heatmap representation of log normalized RMA values from ST1.0 gene microarray (Affymetrix) in all treatment groups of the 20 most differentially expressed genes in SB-3123 following treatment with IFN γ /TNF α (2.4/0.24 ng/mL; C) or vemurafenib (1 μ mol/L; D) relative to untreated SB-3123. SB-3123 was treated for 96 hours in all treatment conditions. Heatmaps show RMA values from three biologically independent gene microarrays for each indicated treatment condition.

explanation as to how vemurafenib co-opts host IFN γ production to mediate tumor regression, namely through increasing tumor sensitivity to the effects of this cytokine.

Despite extensive genetic evidence indicating that provision of vemurafenib enhances SB-3123 sensitivity to a distinct IFN γ /TNF α -driven genetic signature, the specific cytokine-induced genetic changes that mediate the phenotypic observation of reduced SB-3123 growth kinetics remain to be completely elucidated. One specific effector cytokine-induced gene of interest may

be *Casp1*, the gene encoding caspase-1, which is known to be induced by IFN γ in a STAT1-dependent manner and is involved in the induction of apoptosis in multiple tumor types, including breast and pancreatic cancers (38, 39). *Casp1* expression is induced in SB-3123 to a greater level by vemurafenib + IFN γ /TNF α combination treatment relative to IFN γ /TNF α alone (FC = 2.12, P = 5.56E-05; Supplementary Table S11). Another cytokine-responsive gene expressed at a higher level upon combination treatment is the cell-surface death receptor *Fas*

(FC = 1.8, $P = 2.17E-04$; Supplementary Table S11). Increased *Fas* expression may promote tumor cell apoptosis through an auto- or para-Fas:FasL interaction (40). It remains to be determined whether the differential expression of these select genes upon vemurafenib + IFN γ /TNF α treatment is sufficient to mediate the significant reduction in growth kinetics observed in SB-3123. The dramatic phenotypic effects observed with vemurafenib + IFN γ /TNF α provide a basis for further study of the intersection between immunologic and oncogenic signaling in cancer cells and for the rational design of combinatorial approaches to treat patients with melanoma.

As our findings have indicated that BRAF^{V600E} inhibition synergized with T-cell effector cytokines to reduce proliferation of BRAF-mutant human and murine melanomas, it would be very interesting to determine whether the combination of targeted inhibition of oncogenic pathways and T-cell-based immune therapies are synergistic in other cancer histologies. For example, the Btk inhibitor ibrutinib is in development for the treatment of multiple B-cell malignancies (41–44); however, its use as a single agent has been limited because of acquired resistance in the tumor (45, 46). CD19 chimeric antigen receptor immunotherapy is also being developed rapidly as a treatment for CD19-positive B-cell malignancies (47, 48). Perhaps the combination of targeted therapy with ibrutinib + CD19 CAR therapy could mediate superior tumor regressions in comparison with either single strategy for multiple B-cell cancer histologies.

The surprising observation that vemurafenib therapy synergizes with type I cytokines in a BRAF^{V600E} mutation-dependent manner to induce G₁–G₀ cell-cycle arrest has substantial therapeutic implications for the design of clinical trials, as it suggests that optimal synergy between these two therapeutic modalities may depend upon the concurrent long-term maintenance of BRAF oncogenic suppression when combined with T-cell-based immunotherapy. Even though our preclinical findings suggest that in the context of effective antitumor T-cell immunity only concurrent vemurafenib administration may translate into superior clinical efficacy, careful consideration should be given when combined with other immunotherapeutic modalities such as checkpoint inhibitors, which are known to improve endogenous T-cell cytokine production capacity (49). However, clinical data from a recent trial combining the anti-CTLA-4 antibody ipilimumab with vemurafenib strongly argue against a concurrent dosing strategy due to the occurrence of high-grade overlapping toxicities (50). Novel preclinical designs should be considered to better establish

combinatorial schemes to lessen coinciding toxicities without necessarily compromising the overall effectiveness of BRAF inhibition, and the SB-3123 model provides an important experimental tool for such preclinical investigations.

Disclosure of Potential Conflicts of Interest

No potential conflicts of interest were disclosed.

Authors' Contributions

Conception and design: N. Acquavella, D. Clever, D.C. Palmer, Y. Ji, C.A. Klebanoff, R. Roychoudhuri, N.P. Restifo

Development of methodology: N. Acquavella, D. Clever, Z. Yu, M. Roelke-Parker, D.C. Palmer, L. Xi, K.-i. Hanada, F. Marincola, R. Roychoudhuri, N.P. Restifo

Acquisition of data (provided animals, acquired and managed patients, provided facilities, etc.): N. Acquavella, D. Clever, Z. Yu, M. Roelke-Parker, L. Xi, H. Pflücke, A. Gros, Z. Franco, F. Marincola, C.-C.R. Lee, M.W. Bosenberg, N.P. Restifo

Analysis and interpretation of data (e.g., statistical analysis, biostatistics, computational analysis): N. Acquavella, D. Clever, L. Xi, H. Pflücke, Y. Ji, A. Gros, I.S. Goldlust, G.U. Mehta, C.A. Klebanoff, J.G. Crompton, M. Sukumar, J.J. Morrow, L. Gattinoni, E. Wang, F. Marincola, C.-C.R. Lee, M. Raffeld, M.W. Bosenberg, R. Roychoudhuri, N.P. Restifo

Writing, review, and/or revision of the manuscript: N. Acquavella, D. Clever, L. Xi, H. Pflücke, Y. Ji, G.U. Mehta, C.A. Klebanoff, J.G. Crompton, J.J. Morrow, L. Gattinoni, E. Wang, D.F. Stronck, C.-C.R. Lee, M. Raffeld, R. Roychoudhuri, N.P. Restifo

Administrative, technical, or material support (i.e., reporting or organizing data, constructing databases): N. Acquavella, H. Liu, N.P. Restifo

Study supervision: R. Roychoudhuri, N.P. Restifo

Acknowledgments

The authors thank J.R. Wunderlich, S. Xi, and M. Hollingshead (Frederick, MD) for technical advice and thoughtful discussions, E. Tran and D. Jones (Bethesda, MD) for experimental help, T. Hornyak (Baltimore, MD) for providing Melan-a cells, V. Hearing (Bethesda, MD) for providing α -PEP13 antisera, and S. Bates (Bethesda, MD) for providing UACC-62 melanoma cells. The authors especially thank A. "Tito" Fojo, W.L. Dahut, and S.A. Rosenberg (Center for Cancer Research, NIH, Bethesda, MD) for continued support of this project.

Grant support

The authors thank the Milstein Family Foundation for their generous support. This study was also funded by a gift from Li Jinyuan, Chairman of the Tiens Group, NIH-Center for Regenerative Medicine and by the Intramural Research Program of the NCI (ZIA BC010763), Center for Cancer Research, NIH (Bethesda, MD).

Received June 30, 2014; revised October 2, 2014; accepted October 14, 2014; published OnlineFirst November 18, 2014.

References

- Davies H, Bignell GR, Cox C, Stephens P, Edkins S, Clegg S, et al. Mutations of the BRAF gene in human cancer. *Nature* 2002;417:949–54.
- Fecher LA, Amaravadi RK, Flaherty KT. The MAPK pathway in melanoma. *Curr Opin Oncol* 2008;20:183–9.
- Chapman PB, Hauschild A, Robert C, Haanen JB, Ascierto P, Larkin J, et al. Improved survival with vemurafenib in melanoma with BRAF V600E mutation. *N Engl J Med* 2011;364:2507–16.
- Hauschild A, Grob JJ, Demidov LV, Jouary T, Gutzmer R, Millward M, et al. Dabrafenib in BRAF-mutated metastatic melanoma: a multicentre, open-label, phase 3 randomised controlled trial. *Lancet* 2012;380:358–65.
- Sosman JA, Kim KB, Schuchter L, Gonzalez R, Pavlick AC, Weber JS, et al. Survival in BRAF V600-mutant advanced melanoma treated with vemurafenib. *N Engl J Med* 2012;366:707–14.
- Rosenberg SA. Cell transfer immunotherapy for metastatic solid cancer—what clinicians need to know. *Nat Rev Clin Oncol* 2011;8:577–85.
- Rosenberg SA, Yang JC, Sherry RM, Kammula US, Hughes MS, Phan GQ, et al. Durable complete responses in heavily pretreated patients with metastatic melanoma using T-cell transfer immunotherapy. *Clin Cancer Res* 2011;17:4550–7.
- Liu C, Peng W, Xu C, Lou Y, Zhang M, Wargo JA, et al. BRAF inhibition increases tumor infiltration by T cells and enhances the antitumor activity of adoptive immunotherapy in mice. *Clin Cancer Res* 2013;19:393–403.
- Koya RC, Mok S, Otte N, Blacketer KJ, Comin-Anduix B, Tumeh PC, et al. BRAF inhibitor vemurafenib improves the antitumor activity of adoptive cell immunotherapy. *Cancer Res* 2012;72:3928–37.

10. Wilmott JS, Long GV, Howle JR, Haydu LE, Sharma RN, Thompson JF, et al. Selective BRAF inhibitors induce marked T-cell infiltration into human metastatic melanoma. *Clin Cancer Res* 2012;18:1386–94.
11. Frederick DT, Piris A, Cogdill AP, Cooper ZA, Lezcano C, Ferrone CR, et al. BRAF inhibition is associated with enhanced melanoma antigen expression and a more favorable tumor microenvironment in patients with metastatic melanoma. *Clin Cancer Res* 2013;19:1225–31.
12. Knight DA, Ngiew SF, Li M, Parmenter T, Mok S, Cass A, et al. Host immunity contributes to the anti-melanoma activity of BRAF inhibitors. *J Clin Invest* 2013;123:1371–81.
13. Ho PC, Meeth KM, Tsui YC, Srivastava B, Bosenberg MW, Kaech SM. Immune-based antitumor effects of BRAF inhibitors rely on signaling by CD40L and IFN γ . *Cancer Res* 2014;74:3205–17.
14. Boni A, Cogdill AP, Dang P, Udayakumar D, Njauw CN, Sloss CM, et al. Selective BRAFV600E inhibition enhances T-cell recognition of melanoma without affecting lymphocyte function. *Cancer Res* 2010;70:5213–9.
15. Kaplan DH, Shankaran V, Dighe AS, Stockert E, Aguet M, Old LJ, et al. Demonstration of an interferon gamma-dependent tumor surveillance system in immunocompetent mice. *Proc Natl Acad Sci U S A* 1998;95:7556–61.
16. Dighe AS, Richards E, Old LJ, Schreiber RD. Enhanced *in vivo* growth and resistance to rejection of tumor cells expressing dominant negative IFN gamma receptors. *Immunity* 1994;1:447–56.
17. Braumuller H, Wieder T, Brenner E, Assmann S, Hahn M, Alkhaled M, et al. T-helper-1-cell cytokines drive cancer into senescence. *Nature* 2013;494:361–5.
18. Overwijk WW, Theoret MR, Finkelstein SE, Surman DR, de Jong LA, Vyth-Dreese FA, et al. Tumor regression and autoimmunity after reversal of a functionally tolerant state of self-reactive CD8⁺ T cells. *J Exp Med* 2003;198:569–80.
19. Dankort D, Filenova E, Collado M, Serrano M, Jones K, McMahon M. A new mouse model to explore the initiation, progression, and therapy of BRAFV600E-induced lung tumors. *Genes Dev* 2007;21:379–84.
20. Bosenberg M, Muthusamy V, Curley DP, Wang Z, Hobbs C, Nelson B, et al. Characterization of melanocyte-specific inducible Cre recombinase transgenic mice. *Genesis* 2006;44:262–7.
21. Trotman LC, Niki M, Dotan ZA, Koutcher JA, Di Cristofano A, Xiao A, et al. Pten dose dictates cancer progression in the prostate. *PLoS Biol* 2003;1:E59.
22. Harada N, Tamai Y, Ishikawa T, Sauer B, Takaku K, Oshima M, et al. Intestinal polyposis in mice with a dominant stable mutation of the beta-catenin gene. *EMBO J* 1999;18:5931–42.
23. Gartner JJ, Davis S, Wei X, Lin JC, Trivedi NS, Teer JK, et al. Comparative exome sequencing of metastatic lesions provides insights into the mutational progression of melanoma. *BMC Genomics* 2012;13:505.
24. Loewe S, Muischnek H. Effect of combinations: mathematical basis of problem. *Arch Exp Pathol Pharmacol* 1926;114:313–26.
25. Dankort D, Curley DP, Carlidge RA, Nelson B, Karnezis AN, Damsky WE Jr, et al. Braff(V600E) cooperates with Pten loss to induce metastatic melanoma. *Nat Genet* 2009;41:544–52.
26. Damsky WE, Curley DP, Santhanakrishnan M, Rosenbaum LE, Platt JT, Gould Rothberg BE, et al. beta-catenin signaling controls metastasis in Braff-activated Pten-deficient melanomas. *Cancer Cell* 2011;20:741–54.
27. Wagle N, Emery C, Berger MF, Davis MJ, Sawyer A, Pochanard P, et al. Dissecting therapeutic resistance to RAF inhibition in melanoma by tumor genomic profiling. *J Clin Oncol* 2011;29:3085–96.
28. Chin YE, Kitagawa M, Su WC, You ZH, Iwamoto Y, Fu XY. Cell growth arrest and induction of cyclin-dependent kinase inhibitor p21 WAF1/CIP1 mediated by STAT1. *Science* 1996;272:719–22.
29. Bromberg JF, Horvath CM, Wen Z, Schreiber RD, Darnell JE Jr. Transcriptionally active Stat1 is required for the antiproliferative effects of both interferon alpha and interferon gamma. *Proc Natl Acad Sci U S A* 1996;93:7673–8.
30. Johnson JI, Decker S, Zaharevitz D, Rubinstein LV, Venditti JM, Schepartz S, et al. Relationships between drug activity in NCI preclinical *in vitro* and *in vivo* models and early clinical trials. *Br J Cancer* 2001;84:1424–31.
31. Merlino G, Flaherty K, Acquavella N, Day CP, Aplin A, Holmen S, et al. Meeting report: the future of preclinical mouse models in melanoma treatment is now. *Pigment Cell Melanoma Res* 2013;26:E8–E14.
32. Hodis E, Watson IR, Kryukov GV, Arold ST, Imielinski M, Theurillat JP, et al. A landscape of driver mutations in melanoma. *Cell* 2013;150:251–63.
33. Cooper ZA, Juneja VR, Sage PT, Frederick DT, Piris A, Mitra D, et al. Response to BRAF inhibition in melanoma is enhanced when combined with immune checkpoint blockade. *Cancer Immunol Res* 2014;2:643–54.
34. Bollag G, Tsai J, Zhang J, Zhang C, Ibrahim P, Nolop K, et al. Vemurafenib: the first drug approved for BRAF-mutant cancer. *Nat Rev Drug Discov* 2014;11:873–86.
35. Comin-Anduix B, Chodon T, Sazegar H, Matsunaga D, Mock S, Jalil J, et al. The oncogenic BRAF kinase inhibitor PLX4032/RG7204 does not affect the viability or function of human lymphocytes across a wide range of concentrations. *Clin Cancer Res* 2012;16:6040–8.
36. Hong DS, Vence L, Falchook G, Radvanyi LG, Liu C, Goodman V, et al. BRAF(V600) inhibitor GSK2118436 targeted inhibition of mutant BRAF in cancer patients does not impair overall immune competency. *Clin Cancer Res* 2010;18:2326–35.
37. Gray-Schopfer V, Wellbrock C, Marais R. Melanoma biology and new targeted therapy. *Nature* 2007;445:851–7.
38. Detjen KM, Farwig K, Welzel M, Wiedenmann B, Rosewicz S. Interferon gamma inhibits growth of human pancreatic carcinoma cells via caspase-1 dependent induction of apoptosis. *Gut* 2001;49:251–62.
39. Chin YE, Kitagawa M, Kuida K, Flavell RA, Fu XY. Activation of the STAT signaling pathway can cause expression of caspase 1 and apoptosis. *Mol Cell Biol* 1997;17:5328–37.
40. Listopad JJ, Kammertoens T, Anders K, Silkenstedt B, Willmsky G, Schmidt K, et al. Fas expression by tumor stroma is required for cancer eradication. *Proc Natl Acad Sci U S A* 2013;110:2276–81.
41. Byrd JC, O'Brien S, James DF. Ibrutinib in relapsed chronic lymphocytic leukemia. *N Engl J Med* 2013;369:1278–9.
42. Wang ML, Rule S, Martin P, Goy A, Auer R, Kahl BS, et al. Targeting BTK with ibrutinib in relapsed or refractory mantle-cell lymphoma. *N Engl J Med* 2013;369:507–16.
43. Neffendorf JE, Gout I, Hildebrand GD. Ibrutinib in relapsed chronic lymphocytic leukemia. *N Engl J Med* 2013;369:1277.
44. Rushworth SA, MacEwan DJ, Bowles KM. Ibrutinib in relapsed chronic lymphocytic leukemia. *N Engl J Med* 2013;369:1277–8.
45. Woyach JA, Furman RR, Liu TM, Ozer HG, Zapatka M, Ruppert AS, et al. Resistance mechanisms for the Bruton's tyrosine kinase inhibitor ibrutinib. *N Engl J Med* 2014;370:2286–94.
46. Furman RR, Cheng S, Lu P, Setty M, Perez AR, Guo A, et al. Ibrutinib resistance in chronic lymphocytic leukemia. *N Engl J Med* 2014;370:2352–4.
47. Porter DL, Levine BL, Kalos M, Bagg A, June CH. Chimeric antigen receptor-modified T cells in chronic lymphoid leukemia. *N Engl J Med* 2011;365:725–33.
48. Kochenderfer JN, Rosenberg SA. Chimeric antigen receptor-modified T cells in CLL. *N Engl J Med* 2011;365:1937–8.
49. Pardoll DM. The blockade of immune checkpoints in cancer immunotherapy. *Nat Rev Cancer* 2012;12:252–64.
50. Ribas A, Hodi FS, Callahan M, Konto C, Wolchok J. Hepatotoxicity with combination of vemurafenib and ipilimumab. *N Engl J Med* 2013;368:1365–6.

Cancer Immunology Research

Type I Cytokines Synergize with Oncogene Inhibition to Induce Tumor Growth Arrest

Nicolas Acquavella, David Clever, Zhiya Yu, et al.

Cancer Immunol Res 2015;3:37-47. Published OnlineFirst October 30, 2014.

Updated version Access the most recent version of this article at:
doi:[10.1158/2326-6066.CIR-14-0122](https://doi.org/10.1158/2326-6066.CIR-14-0122)

Supplementary Material Access the most recent supplemental material at:
<http://cancerimmunolres.aacrjournals.org/content/suppl/2014/10/30/2326-6066.CIR-14-0122.DC1>

Cited articles This article cites 50 articles, 17 of which you can access for free at:
<http://cancerimmunolres.aacrjournals.org/content/3/1/37.full#ref-list-1>

Citing articles This article has been cited by 4 HighWire-hosted articles. Access the articles at:
<http://cancerimmunolres.aacrjournals.org/content/3/1/37.full#related-urls>

E-mail alerts [Sign up to receive free email-alerts](#) related to this article or journal.

Reprints and Subscriptions To order reprints of this article or to subscribe to the journal, contact the AACR Publications Department at pubs@aacr.org.

Permissions To request permission to re-use all or part of this article, use this link
<http://cancerimmunolres.aacrjournals.org/content/3/1/37>.
Click on "Request Permissions" which will take you to the Copyright Clearance Center's (CCC) Rightslink site.